

**GT2011-45122**

**LAMINAR FLAME SPEED MEASUREMENTS AND MODELING OF ALKANE BLENDS AT  
ELEVATED PRESSURES WITH VARIOUS DILUENTS**

**Yash Kochar, Jerry Seitzman and Timothy Lieuwen**  
School of Aerospace Engineering  
Georgia Institute of Technology, Atlanta, GA, USA

**Wayne Metcalfe, Sinéad Burke and Henry Curran**  
Combustion Chemistry Centre and School of Chemistry  
NUI Galway, University Road, Galway, Ireland

**Michael Krejci, William Lowry and Eric Petersen**  
Department of Mechanical Engineering  
Texas A&M University, College Station, TX, USA

**Gilles Bourque**  
Rolls-Royce Canada, Montreal, Canada

**ABSTRACT**

Laminar flame speeds at elevated pressure for methane-based fuel blends are important for refining the chemical kinetics that are relevant at engine conditions. The present paper builds on earlier measurements and modeling by the authors by extending the validity of a chemical kinetics mechanism to laminar flame speed measurements obtained in mixtures containing significant levels of helium. Such mixtures increase the stability of the experimental flames at elevated pressures and extend the range of laminar flame speeds. Two experimental techniques were utilized, namely a Bunsen burner method and an expanding spherical flame method. Pressures up to 10 atm were studied, and the mixtures ranged from pure methane to binary blends of  $\text{CH}_4/\text{C}_2\text{H}_6$  and  $\text{CH}_4/\text{C}_3\text{H}_8$ . In the Bunsen flames, the data include elevated initial temperatures up to 650 K. There is generally good agreement between model and experiment, although some discrepancies still exist with respect to equivalence ratio for certain cases. A significant result of the present study is that the effect of mixture composition on flame speed is well captured by the mechanism over the extreme ranges of initial pressure and temperature covered herein. Similarly, the mechanism does an excellent job at modeling the effect of initial temperature for methane-based mixtures up to at least 650 K.

**INTRODUCTION**

Because of its importance to chemical kinetic mechanism development and gas turbine combustion, laminar flame speed continues to be a topic of active research [1]–[4]. Mixtures of methane, ethane, and propane are of particular interest because they are the primary components of natural gas-based fuels for

power generation gas turbine engines. Recent work by the authors has concentrated on the use of laminar flame speeds of binary fuel blends at elevated pressure to validate a modern chemical kinetics mechanism [1]. However, at elevated pressures, premixed laminar flames become highly susceptible to thermal and hydrodynamic instabilities, therefore limiting the practical experimental limits of observation. One method for extending the stable limits of laminar flame propagation at elevated pressures is to replace some or all of the nitrogen in the fuel-air mixture with helium [5]–[7]. The present study focuses on recent experiments and modeling of high-pressure laminar flame speeds of methane-based blends in the presence of a helium diluent.

As a part of this study, an improved version of a C4 chemical kinetics model [8]–[11] was developed by the authors. It includes 228 species and 1,324 reactions. Two complementary methods are employed here to measure flame speeds. The first is a spherical flame speed approach employing a constant volume combustion-bomb performed at Texas A&M University (TAMU). Using this approach, both un-stretched laminar flame speeds and Markstein lengths can be determined. The second measurement approach utilizes a laminar jet flame and measurement of the burned flame area using imaging of the chemiluminescence emissions performed at Georgia Institute of Technology (GT). This approach for measuring laminar flame speed, which has been validated previously for  $\text{H}_2$  and hydrocarbon fuels [12], provides access to higher temperatures than typically attainable in the spherical flame approach. Provided in this paper are brief overviews of both experimental techniques (bomb and Bunsen flame), followed by an overview of the kinetic mechanism and the recent improvements made to it. Results from the experiments

for the pure methane and ethane cases are summarized first, and the results for the methane-ethane and methane-propane blends provided second.

## EXPERIMENTAL SETUP

### Design and Hardware (TAMU)

A constant-volume cylindrical vessel made from 7075-T6 aluminum alloy was used to perform the experiments within this study. The vessel's basic dimensions are an interior diameter of 30.5 cm, an outer diameter of 38.1 cm, and an internal length of 35.6 cm. Two 20-cm diameter, 6.35-cm thick fused quartz windows, which are clamped between neoprene gaskets with stainless steel spacers, provide a 12.7-cm diameter optical port through the vessel.

Gas	Grade	Purity
CH <sub>4</sub>	3.7	99.97%
C <sub>2</sub> H <sub>6</sub>	3.5	99.95%
C <sub>3</sub> H <sub>8</sub>	Instrument	99.5%
O <sub>2</sub>	UHP	99.999%
N <sub>2</sub>	UHP	99.999%
He	UHP	99.999%

All mixtures were made using the partial pressure method either directly in the vessel or in a separate, stainless steel mixing tank. The purity of the gases used in the present study and referenced from previous studies is summarized in Table 1. Further details on the facility are provided in de Vries [13].

A Z-type Schlieren system was used to monitor the expansion of the flame. Figure 1 shows a schematic of the optical setup, which is similar to that suggested by Settles [14]. The system has f/8 optics throughout, with 15.2-cm diameter parabolic mirrors. A circular pinhole aperture was found in earlier studies by the authors to resolve the image better than a vertical knife edge [4]. The images were recorded using a high-speed camera.

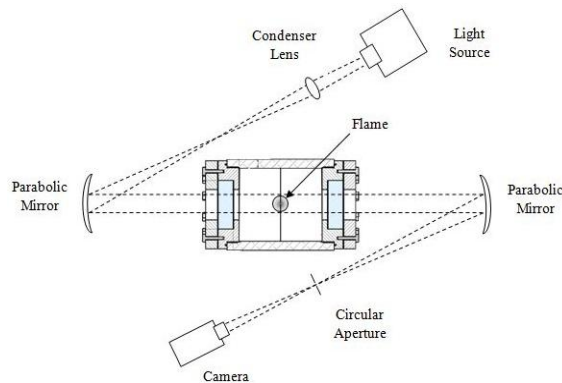


Figure 1: Optical setup for high-speed schlieren system.

Figure 2 shows sample images from this study; these images demonstrate the quality of images taken and show the continuous laminar behavior of a 10-atm initial pressure methane-helium mixture. The time step in Figure 2 is normalized to the first image presented.

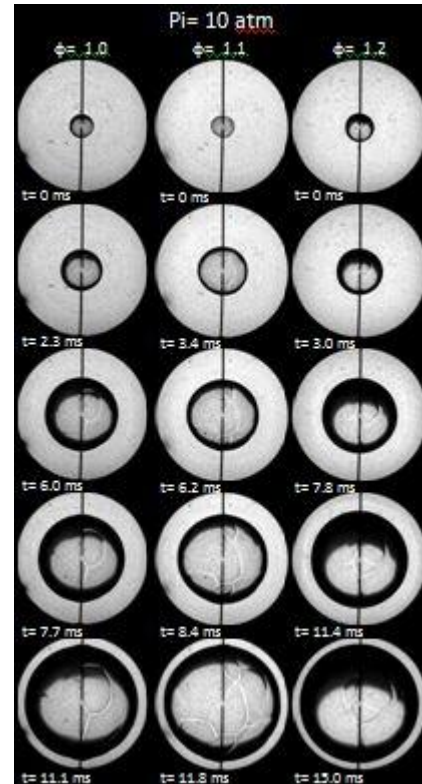


Figure 2: Flame images for 10-atm pure CH<sub>4</sub> with a 1:6 O<sub>2</sub>:He at  $\phi=1.0$  (left),  $\phi=1.1$  (middle), and  $\phi=1.2$  (right).

### Bunsen Flame Facility (GT)

A schematic of the second experimental facility used for flame speed measurements with the modified Bunsen flame technique is shown in Figure 3. The facility produces axisymmetric jet flames using contoured laminar nozzle. The reactant gas flow rates are measured individually using a bank of rotameters and allowed sufficient residence time to mix thoroughly before passing through the nozzle. The rotameters are calibrated for the desired flow rate range, at the supply pressure, using a wet test meter for high flow rates and a bubble flow meter for low flow rates. Overall, the flow rate calibration has an accuracy of better than 1%.

The reactant mixture passes through a plenum where it is preheated to the desired temperature with electric resistance heaters. The temperature of the reactants is monitored with a K-type thermocouple placed 25 mm upstream of the exit. The exit diameter of the contoured burner is 9 mm. A sintered plate surrounding the nozzle exit is used to produce a near-stoichiometric, flat, methane-air pilot flame. The pilot flame helps to anchor the flame at high flow rates. The complete

burner assembly is placed in a nitrogen ventilated pressure chamber. The pressure chamber can withstand up to 30 bar pressure at a wall temperature of 500 K (which is well above the typical wall temperature during operation).

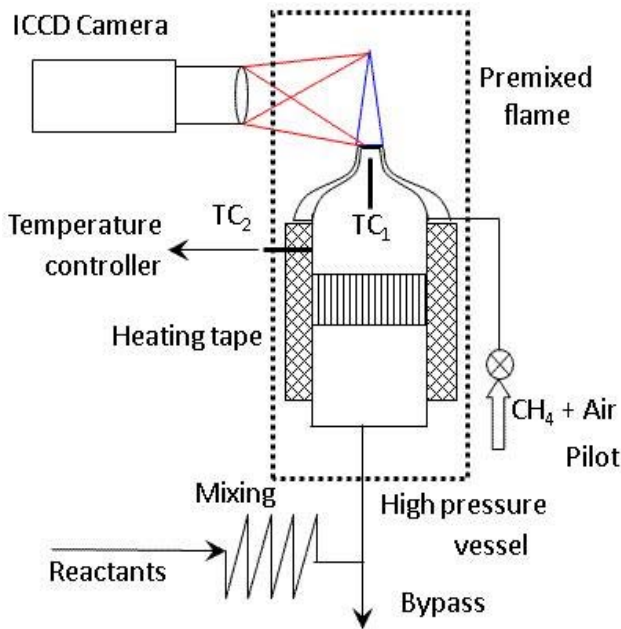


Figure 3: Schematic of the experimental setup.

Optical access for flame imaging is provided by three, 25.4-mm diameter quartz windows. Broadband chemiluminescence images of the Bunsen flame are acquired using a 16-bit ICCD camera attached with  $f/4.5$ , 105 mm UV Nikkor lens. The camera is sensitive in the visible and ultraviolet range and capable of capturing  $\text{CH}^*$ ,  $\text{OH}^*$  and  $\text{CO}_2^*$  chemiluminescence from the flame. The magnification of the imaging system ranged from  $\sim 30$ – $50 \mu\text{m}/\text{pixel}$ .

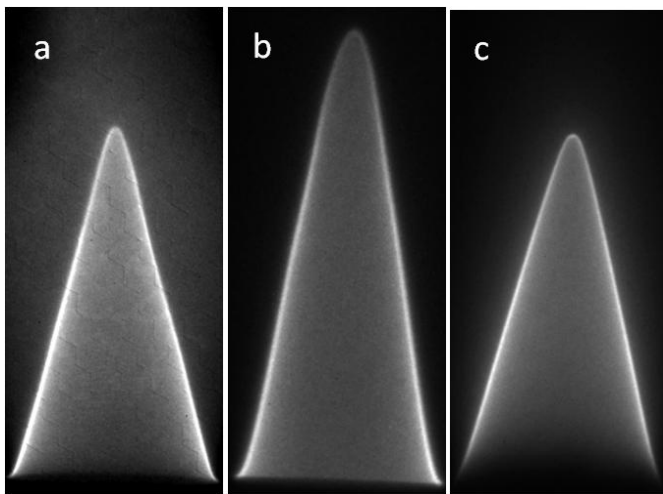


Figure 4: Instantaneous images of the flame. (a)  $\text{CH}_4\text{-O}_2\text{:He}$  (1:5), 10 atm, 326 K,  $\Phi=0.86$ , (b)  $\text{C}_2\text{H}_6\text{-air}$ , 5 atm, 333 K,  $\Phi=0.86$ , (c)  $\text{C}_3\text{H}_8\text{-air}$ , 1 atm, 650 K,  $\Phi=0.87$ .

Example flame images are shown in Figure 4 for a range of fuels and pressures. The image exposure times are a few milliseconds, and reveal the flames to be essentially axisymmetric and stable.

The chemiluminescence images are analyzed to determine the reaction zone location with a gradient-based edge detection algorithm. The algorithm finds the inner edge of the reaction zone for both the left and right half images, from which the reaction zone area. The reaction zone areas from 50 realizations are then averaged to determine the flame area ( $A_b$ ) at each operating condition. The unstretched, unburned flame

speed ( $S_L$ ) can then be calculated from,  $S_L = \frac{\dot{Q}}{A_b}$ , where  $\dot{Q}$  is the measured volumetric flow rate of the reactants. This procedure, which involves determining the reaction zone area as opposed to the inner edge of the preheat zone has been shown to provide a better estimate of the unstretched (1-d) flame speed, as it is only weakly affected by the flame curvature and because the Bunsen flame strain is primarily restricted to the low area flame tip [12].

### Modeling

A chemical kinetic mechanism was developed and simulations performed using the Premix module in the CHEMKIN-PRO package[15]. The detailed chemical kinetics mechanism is based on the hierarchical nature of hydrocarbon combustion mechanisms containing the  $\text{H}_2/\text{O}_2$  sub-mechanism [8], together with the  $\text{CO}/\text{CH}_4$  and the  $\text{C}_2$  and  $\text{C}_3$  sub-mechanisms that have already been published [9]–[11]. The  $\text{C}_4$  sub-mechanism has been fully detailed in two recent papers on the butane isomers [16], [17]. The current mechanism version is denoted C4\_52.0\_LT, containing 228 species and 1324 reactions, which is an update from the mechanism previously presented by some of the authors describing laminar flame speeds of pure and blended alkanes [1]. This mechanism contains detailed chemistry describing both the high and low temperature combustion pathways of  $\text{C}_1$  to  $\text{C}_4$  hydrocarbons. As the species involved in these low temperature pathways (e.g. alkylperoxy radicals, hydroperoxyl-alkyl radicals, ketohydroperoxide species etc.) are not formed at the elevated temperatures encountered in the flame environment, they have been removed from the mechanism, together with their reactions, resulting in a significant decrease in the computational time required to converge the flame speed simulations. Two mechanisms resulted from the process, C3\_52.0\_HT, and C4\_52.0\_HT containing reactions describing the high temperature combustion of the relevant hydrocarbons, namely  $\text{C}_1\text{-C}_3$  and  $\text{C}_1\text{-C}_4$ . All three mechanisms were seen to provide almost identical predictions of flame speed (ca.  $< 0.2 \text{ cm s}^{-1}$  difference) for a variety of different fuel mixtures and initial conditions, identifying no loss of accuracy with the decreasing computational cost. Almost all of the calculations shown below were performed with the C3\_52.0\_HT version of the mechanism, containing

94 species and 583 reactions. There has been several updates to the mechanism from our previous work [1], based on further improving the agreement with the methane, ethane, propane data presented in [1] and a concurrent extensive modeling and experimental effort to increase our knowledge of various C<sub>0</sub>-C<sub>4</sub> fuels.

**Table 2: Updated rate coefficients in mechanism version C4\_52.0\_LT. cm<sup>3</sup> mol<sup>-1</sup> s<sup>-1</sup> cal<sup>-1</sup> units.**

Reaction	A	n	Ea	Ref.
H+O <sub>2</sub> ⇌O+OH	9.65E+14	- 0.26	16200.	[18]
H <sub>2</sub> O <sub>2</sub> (+M)⇌OH+OH(+M)	8.59E+14	0.00	48560.	[18]
LOW	9.55E+15	0.00	42203.	
TROE 1.0 1.0E+30 1.0E+30				
N <sub>2</sub> /1.5/H <sub>2</sub> O/9.0/				
H <sub>2</sub> O <sub>2</sub> +OH⇌H <sub>2</sub> O+HO <sub>2</sub>	1.74E+12	0.00	318.	[18]
H <sub>2</sub> O <sub>2</sub> +OH⇌H <sub>2</sub> O+HO <sub>2</sub>	7.59E+13	0.00	7269.	
CO+HO <sub>2</sub> ⇌CO <sub>2</sub> +OH	1.57E+05	2.18	17940.	[19]
CH <sub>2</sub> +O <sub>2</sub> ⇌HCO+OH	1.06E+13	0.00	1500.	[20]
CH <sub>2</sub> +O <sub>2</sub> ⇌CO <sub>2</sub> +H+H	2.64E+12	0.00	1500.	[20]
C <sub>2</sub> H <sub>6</sub> +O <sub>2</sub> ⇌C <sub>2</sub> H <sub>5</sub> +HO <sub>2</sub>	6.03E+13	0.00	51870.	[21]
HCCO+O <sub>2</sub> ⇌OH+CO+CO	1.91E+11	- 0.02	1020.	[22]
HCCO+O <sub>2</sub> ⇌CO <sub>2</sub> +CO+H	4.78E+12	- 0.14	1150.	[22]
C <sub>2</sub> H <sub>6</sub> +HO <sub>2</sub> ⇌C <sub>2</sub> H <sub>5</sub> +H <sub>2</sub> O <sub>2</sub>	6.92E+01	3.61	16920.	[23]
C <sub>2</sub> H <sub>5</sub> (+M)⇌C <sub>2</sub> H <sub>4</sub> +H(+M)	1.11E+10	1.04	36769.	[24]
LOW	3.99E+33	- 4.99	40000.	
TROE 0.168 1203.0 0.0				
H <sub>2</sub> /2.0/ H <sub>2</sub> O/6.0/ CH <sub>4</sub> /2.0/ CO/1.5/ CO <sub>2</sub> /2.0/ Ar/0.7/				
CH <sub>3</sub> +CH <sub>3</sub> (+M)⇌C <sub>2</sub> H <sub>5</sub> +H(+M)	4.99E12	0.10	1060.	[25]
HIGH	3.80E-7	4.84	7710.	
SRI 1.641 4334.0 2725.0				
C <sub>2</sub> H <sub>5</sub> +O <sub>2</sub> ⇌C <sub>2</sub> H <sub>4</sub> +HO <sub>2</sub>	3.78E+14	- 1.01	4749.	[26]
CH <sub>3</sub> CO(+M)⇌CH <sub>3</sub> +CO(+M)	1.07E+12	0.63	16900.	[27]
LOW	5.65E+18	- 0.97	14600.	
TROE 0.629 8.73E+09 5.52 7.60E+07				
CH <sub>2</sub> CHO(+M)⇌CH <sub>2</sub> CO+H(+M)	1.43E+15	- 0.15	45600.	[27]
LOW	6.00E+29	-3.8	43424.	
TROE 0.985 393.0 9.80E+09 5.00E+09				
CH <sub>2</sub> CHO(+M)⇌CH <sub>3</sub> +CO(+M)	2.93E+12	0.29	40300.	[27]
LOW	9.52E+33	- 5.07	41300.	
TROE 7.13E-17 1.15E+03 4.99E+09 1.79E+09				
C <sub>2</sub> H <sub>4</sub> +O⇌CH <sub>3</sub> +HCO	6.78E+06	1.88	183.	[28]
C <sub>2</sub> H <sub>4</sub> +O⇌CH <sub>2</sub> CHO+H	6.78E+06	1.88	183.	[28]
C <sub>2</sub> H <sub>4</sub> +O <sub>2</sub> ⇌C <sub>2</sub> H <sub>3</sub> +HO <sub>2</sub>	4.22E+13	0.00	57623.	[29]
C <sub>2</sub> H <sub>4</sub> +CH <sub>3</sub> O <sub>2</sub> ⇌C <sub>2</sub> H <sub>3</sub> +CH <sub>3</sub> O <sub>2</sub> H	8.59E+00	3.75	27132.	[30]
C <sub>2</sub> H <sub>4</sub> +C <sub>2</sub> H <sub>5</sub> O <sub>2</sub> ⇌C <sub>2</sub> H <sub>3</sub> +C <sub>2</sub> H <sub>5</sub> O <sub>2</sub> H	8.59E+00	3.75	27132.	[30]
C <sub>2</sub> H <sub>4</sub> +HO <sub>2</sub> ⇌C <sub>2</sub> H <sub>4</sub> O1-2+OH	1.12E+12	0.0	17190.	Est.
C <sub>2</sub> H <sub>3</sub> +O <sub>2</sub> <=>CH <sub>2</sub> O+HCO	1.70E+29	- 5.31	6503.	[31]
C <sub>2</sub> H <sub>3</sub> +O <sub>2</sub> <=>CH <sub>2</sub> CHO+O	7.00E+14	- 0.61	5262.	[31]
C <sub>2</sub> H <sub>3</sub> +O <sub>2</sub> <=>C <sub>2</sub> H <sub>2</sub> +HO <sub>2</sub>	5.19E+15	- 1.26	3313.	[31]

All of the relevant updates to the mechanism are shown in Table 2 while the most important updates will be discussed in the text.

The mechanism undergoes simultaneous optimization to many relevant datasets. These include low temperature, high pressure rapid compression machine ignition delay time measurements of hydrogen/oxygen mixtures and methane/air mixtures, shock tube ignition delays measurements of methane, ethane (and their mixtures), ethylene, and dimethyl ether, and also laminar flame speed measurements of acetylene and acetone. These particular C<sub>0</sub>-C<sub>4</sub> components are highlighted as their investigations have resulted in the improvements in performance of the C<sub>4</sub> mechanism from that presented in [1]. It also highlights the importance of validating a mechanism against a wide range of targets, leading to a globally applicable C<sub>0</sub>-C<sub>4</sub> mechanism. The mechanism has not been optimized using any of the new data presented in this work, namely the flame speeds measured at elevated temperatures and diluted in helium.

The H<sub>2</sub>/O<sub>2</sub> sub-mechanism was updated based on recent work by Hong *et al.* [18]. The rate constant recommended for the very important chain branching reaction between atomic hydrogen and molecular oxygen producing two reactive radicals in the form of oxygen atom and hydroxyl radical has been adopted from this work. Hong *et al.* also recommend values for the pressure dependant decomposition of hydrogen peroxide to form two hydroxyl radicals, and this expression has also been integrated into the current version of the mechanism.

The pressure-dependant decomposition of ethyl radical is a very important reaction in the combustion of ethane and ethylene, and thus many larger hydrocarbon fuels. In our previous work [1] the detailed description from Miller and Klippenstein [32] was adopted which improved the mechanism predictions of ethane/air flame speed. However, when validating the mechanism against methane/ethane shock tube ignition delay data and ethylene shock tube ignition delay data, the Miller and Klippenstein description of ethyl decomposition caused a large increase in reactivity that could not be reconciled with the current kinetic scheme. Their description is the product of a very detailed computational analysis and is very well validated against low pressure data, but in the pressure range of the aforementioned ignition delay studies (approximately 1-30 atm) it caused an over-prediction in reactivity. Efforts are continuing to solve this anomaly, but in order to have a robust mechanism applicable to engine relevant conditions a different description [24] has been adopted.

A chemically activated description of the reaction between two methyl radicals to form ethyl radical and hydrogen atom has been adopted from Stewart *et al.* [25] to improve the predicted pressure dependence observed experimentally in the

room temperature, methane/air and ethane/air flame speed measurements.

An important improvement to the ethylene sub-mechanism was made by adopting the pressure dependant decomposition of the  $\text{CH}_2\text{CHO}$  radical from the work of Senosiain *et al.* [27] and the recommendation of Baulch *et al.* [28] for the reaction between ethylene and atomic oxygen. The branching ratios of both these channels were slightly adjusted to improve agreement with ethylene/air shock-tube ignition delay measurements, with the adjusted values shown in Table 2.

Finally, the authors would like to highlight some issues encountered during the simulation of the helium-diluted mixtures. As mentioned previously, the simulations were performed using the Premix module of Chemkin Pro. As a check of the validity of a flame speed calculation, it is routine to ensure that the final temperature calculated by Premix at a large distance from the burner is equal to the adiabatic flame temperature of the relevant mixture. This is a good test of the level of convergence of the solution and for the nitrogen diluted mixtures the agreement between these two temperatures was excellent, within a fraction of a degree. However, for the helium diluted cases, and in particular for the ethane and propane containing mixtures, the final temperature predicted by Premix was constantly approximately ten degrees higher than the relevant adiabatic flame temperature. This issue was found to be independent of mechanism and thermochemistry and present even if the solution was solved using a very fine mesh (>1500 grid points) and a very large domain (XEND–XSTR = 120 cm).

Based on a limited analysis, it is estimated that the calculated flame speeds should be approximately  $1.0 \text{ cm s}^{-1}$  lower than presented for the helium-diluted experiments.

## RESULTS

A list of conditions and mixture compositions presented in this work is summarized in Table 3.

**Table 3: Mixture compositions and experimental conditions presented in this study.**

Mixture %			Diluent	$\Phi$	$T_u$ (K)	$P_i$ (atm)	Facility
$\text{CH}_4$	$\text{C}_2\text{H}_6$	$\text{C}_3\text{H}_8$					
100	0	0	$\text{O}_2(1):\text{He}(5)$	0.8–1.2	$\approx 298$	10.0	TAMU
0	100	0	Air	0.7–1.2	$\approx 325$	5.0	GT
80	20	0	$\text{O}_2(1):\text{He}(6)$	0.6–1.2	$\approx 600$	5 & 10	GT
60	40	0	$\text{O}_2(1):\text{He}(6)$	0.6–1.2	$\approx 305$ & 600	5.0	GT
80	20	0	$\text{O}_2(1):\text{He}(6)$	1.0	$\approx 298$ & 600	5 & 10	GT & TAMU
60	40	0	$\text{O}_2(1):\text{He}(6)$	1.0	$\approx 298$ & 600	5 & 10	GT & TAMU

80	0	20	$\text{O}_2(1):\text{He}(6)$	1.0	$\approx 298$ & 600	5.0	GT & TAMU
60	0	40	$\text{O}_2(1):\text{He}(6)$	1.0	$\approx 298$ & 600	5.0	GT & TAMU

## Methane

Figure 5 shows the results for the pure methane study performed at TAMU [1] and at GT [33] against the experimental work done by Aung *et al.* [34]; Hassan *et al.* [35]; Vagelopoulos and Egolopoulos [36]; Gu *et al.* [37]; Rozenchan *et al.* [38]; Bosschaart and de Goey [39]; and Tahtouh *et al.* [40].

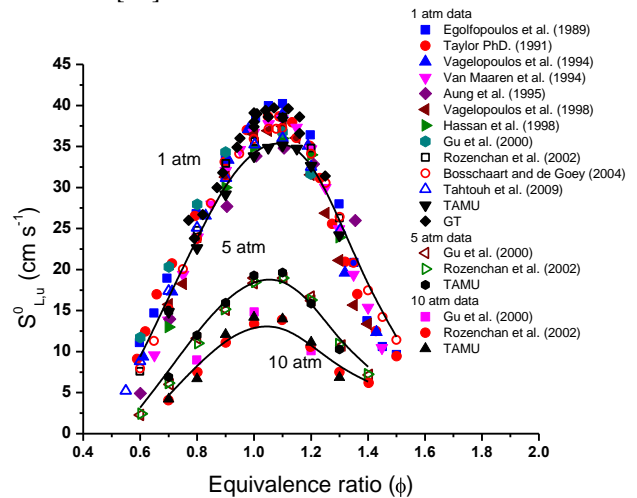


**Figure 5: Methane laminar flame speed results in air at 1, 5 and 10 atm. Points are experimental results, lines are model predictions.**

This figure is included to show how flame speed data taken in the authors’ experimental facilities compare with literature data as a function of both equivalence and pressure under “conventional” fuel in air conditions.

Predictions of the chemical kinetic model are also included. At 1 atm there is a remarkable spread in maximum measured flame speed between  $35$  and  $40 \text{ cm s}^{-1}$  (or nearly  $\pm 10\%$ ) at an equivalence ratio of between 1.05 and 1.1. This may be partly due to problems with flame stretch not being accounted for in earlier measurements. The experimental data from TAMU at 1-atm is slower compared to the other literature data while that from GT is on the faster side. At 5- and 10-atm the TAMU data agrees well with the data of Gu *et al.* [37] and Rozenchan *et al.* [38], certainly within the 1-cm/s uncertainty in the measured flame speeds. The results are internally consistent and follow the expected trend of decreasing flame speed with increasing pressure. In addition, the model agrees quite well with the data and captures the pressure dependence very well.

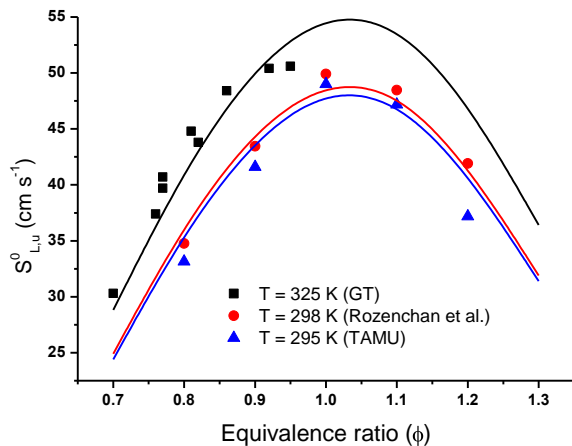


**Figure 6: Methane laminar flame speed results with  $O_2 / He$  (1:5) diluent at  $p = 10$  atm. Points are experimental results, lines are model predictions.**

Figure 6 shows comparisons of experimental results for pure methane at an  $O_2:He$  ratio of 1:5 at 10-atm and at unburned gas temperatures of 295, 298 and 325 K. Here it can be seen that as the temperature increases so does the flame speed, throughout the equivalence ratio range.

Comparing the experimental TAMU data recorded at 295 K with that of Rozenchan et al. [38] measured at 298 K (only a  $3^\circ C$  difference) it is possible to observe the effect of unburned gas temperature both in the experimental results and model predictions. The model captures well the sensitivity of flame speed to both the unburned gas temperature and the equivalence ratio.

In addition, the higher reactant temperature data recorded at GT [33] are well simulated by the model, which again shows the effect of reactant preheat temperature on flame speed; significantly faster flame speeds are observed at 325 K compared to 295/298 K. The data are available only under lean conditions but the calculations have been extended to rich conditions to indicate the overall behavior.

### Ethane

Figure 7 presents the pure ethane results taken in the TAMU facility [1] against the experimental work of Aung et al. [34]; Vagelopoulos and Egolfopoulos [36]; Konnov et al. [41]; Bosschaart and de Goey [39]; Jomaas et al. [42]; Dyakov et al. [43]; and the authors' kinetics model at 1-, 5- and 10-atm with an unburned gas temperature of 295–298 K. The atmospheric-ethane results show that there is good agreement between the data presented herein and previously published results.

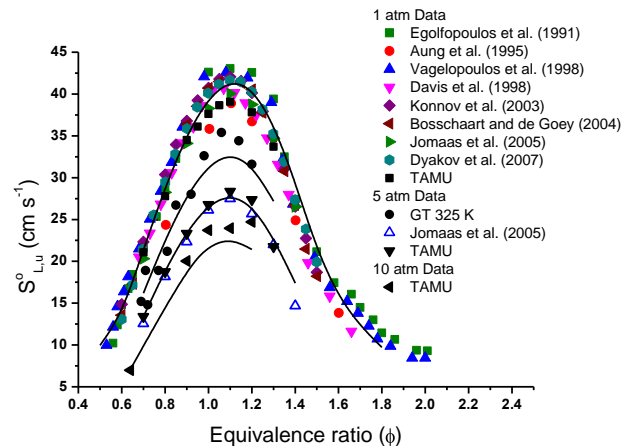


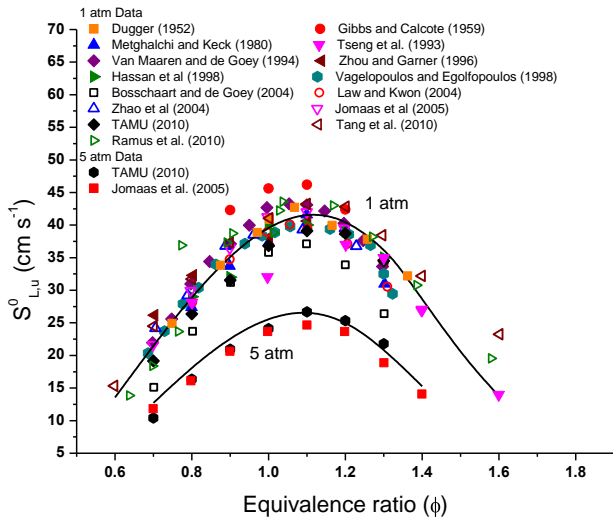
**Figure 7: Ethane laminar flame speed results in air at 1, 5 and 10 atm. Points are experimental results, lines are model predictions.**

Again the data measured at TAMU is slightly slower than that taken in other facilities at 1-atm. However, the results from Jomaas et al. [42] agree well with the TAMU study across the range of experiments at 1- and 5-atm. In addition, the model shows good agreement with the experimental data at 1- and 5-atm. Moreover the ability of the model to accurately capture the influence of reactant temperature is seen in the agreement with the GT data, which was taken at an unburned gas temperature of 325 K, even though it does under-predict the peak flame speeds measured at GT for equivalence ratios in the range 1.0–1.2.

The experimental results of the pure-ethane mixtures at 10 atm at TAMU are also under-predicted by the model, where predicted flame speeds are about 20% lower than the experiments at their peak in the range  $\phi = 1.0$ –1.2.

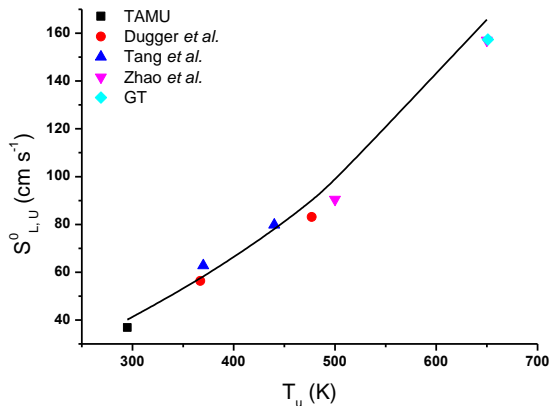
### Propane

Figure 8 presents the pure propane results taken in the TAMU facility [1] compared to the experimental work of Vagelopoulos and Egolfopoulos [36]; Zhao et al. [44]; Jomaas et al. [42]; Gibbs and Calcote [45]; Bosschaart and de Goey [39]; Dugger et al.[46]; Van Maaren and De Goey [47]; Hassan et al. [48]; Metghalchi and Keck [49]; Zhou and Garner [50] Law and Kwon [51]; Tang et al. [52]; Tseng [53] and Razus et al. [54] all taken at an unburned gas temperature of 298 K.



**Figure 8: Propane laminar flame speed results in air at 1- and 5-atm. Points are experimental results, lines are model predictions.**

It is evident that at 1 atm there is considerable scatter in the data, largely due to earlier data having problems with flame stretch and facilities being less sophisticated. However, there is good agreement between the recent work performed at TAMU and that performed by Vagelopoulos and Egolfopoulos [36], Jomaas et al. [42], Zhou and Garner [50], Law and Kwon [51] and Tseng et al. [53]. At 5 atm there is very good agreement between the TAMU data and the data of Jomaas et al. At both 1- and 5-atm the model agrees well with the experimental data.



**Figure 9: Effect of unburned gas temperature on  $C_3H_8$  laminar flame speed for undiluted mixtures in air at  $\phi = 1.0$ ,  $P = 1$  atm. Points are experimental results, line is model prediction.**

Figure 9 depicts the effect of unburned gas temperature on flame speed at  $\phi = 1.0$  and at 1-atm pressure for data taken from the work of Zhao et al. [44], Tang et al. [52], Razus et al. [54], Dugger et al. [46] and from the laboratories at TAMU [1] and GT [33].

The experimental data show that there is a strong positive dependence of measured flame speed on temperature and this

is accurately captured by the model. At approximately 300 K the flame speed is measured to be  $40 \text{ cm s}^{-1}$ , rising to approximately  $160 \text{ cm s}^{-1}$  at 650 K. Where experimental data overlap at approximately 360 K for Tang et al. and Dugger et al. and at 650 K for Zhou and Garner and the GT data there is also very good agreement.

## Fuel Mixtures

The fuel blend studies consisted of 80%/20% and 60%/40% splits of methane/ethane, and methane/propane on a volume basis, performed at varying initial pressures and temperatures. In addition, the oxidizer for these cases was a 1:6 mixture of  $O_2$ :He, and represent the first flame speed measurements of such blends. Helium was used as a diluent to suppress flame instabilities in the experiments at the high-pressure operating conditions. The ratio of  $O_2$  to He was chosen to produce nearly the same adiabatic flame temperatures as fuel-air mixtures. For example, the adiabatic flame temperature of a stoichiometric mixture of 80% methane and 20% ethane with air at 5 atm and 300 K reactant temperature is  $\sim 2270$  K. For the same conditions employing the He: $O_2$  oxidizer, the adiabatic flame temperature is 7 K higher. Generally the difference is less than 10K between air and He: $O_2$  oxidizer for the conditions of this study.

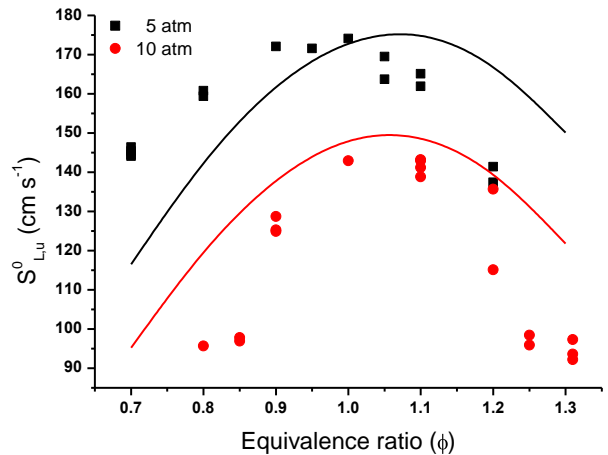


**Figure 10: 80%  $CH_4$  / 20%  $C_2H_6$  laminar flame speed results with  $O_2$ :He (1:6) diluent,  $T_u \approx 600$  K taken at GT. Points are experimental results, lines are model predictions.**

Figure 10 shows experimental results for an 80% methane/20% ethane mixture at high reactant temperature ( $\sim 600$ K) and high pressure (5- and 10-atm). At 5-atm, the experimental results show a peak in flame speed slightly on the rich side, which is similar to other data diluted in air and measured at lower pressure. At both 5- and 10-atm, the decrease in flame speed as a function of equivalence ratio for rich mixtures is observed to be steeper in the experiments compared to the model predictions. This equivalence ratio trend is feature of all of the data taken at high pressure for rich mixtures of methane with both ethane and propane. Overall

the model produces flame speeds that are slightly faster than the experimental results but captures the qualitative features. The shape of the variation in measured flame speed as a function of equivalence ratio is well reproduced.

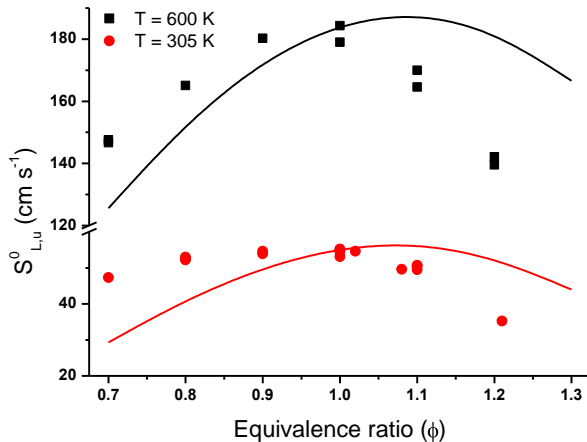


**Figure 11: 60% CH<sub>4</sub> / 40% C<sub>2</sub>H<sub>6</sub> laminar flame speed results with O<sub>2</sub> / He (1:6) diluent, P = 5 atm taken at GT (305 and 600 K). Points are experimental results, lines are model predictions.**

Figure 11 shows results for a mixture with higher ethane content (60% methane/40% ethane) at low and high preheat temperatures (305 and 600 K) and 5-atm. As in the lower ethane content case, there is reasonable agreement between the model and the experimental results. The overall shape and peak flame speeds found in the experimental data are well-matched by the model results. As before, however, the experimental results appear to be slightly shifted to the lean side. This systematic discrepancy between the jet flame data and the model results is found to different extents in all the helium diluted cases. The source of the discrepancy has been investigated. For example, the estimated uncertainties in the experimental determination of mixture equivalence ratio and He dilution level were examined, and different approaches were used to calibrate the flow metering system used in the experiments. However, the estimated uncertainties (given in the Experimental Setup section) are insufficient to explain the observed discrepancies.

Figure 12 furthers the discussion of blending ratio for the helium-diluted flames by showing the effect of decreasing the methane concentration on flame speed for mixtures of both methane-ethane and methane-propane. Figure 12 shows results for stoichiometric fuel-oxidizer mixtures. The data from both facilities show a decrease in flame speed with increasing methane concentration from 60–80% at both low and high temperatures and at 5 and 10 atm.

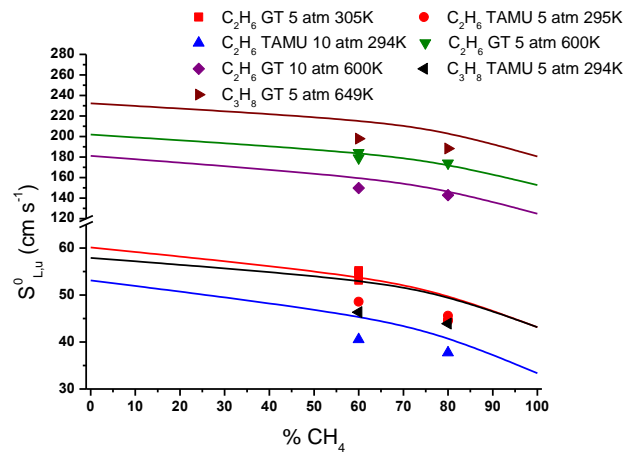


**Figure 12: Influence of mixture composition on laminar flame speed results for CH<sub>4</sub>/C<sub>2</sub>H<sub>6</sub> and CH<sub>4</sub>/C<sub>3</sub>H<sub>8</sub> mixtures with O<sub>2</sub> / He (1:6) diluent, p = 5 and 10 atm, T<sub>u</sub> ≈ 300 and 600 K, φ = 1.0 taken in the two facilities. Points are experimental results, lines are model predictions.**

The results from the different facilities compare quite well with each other at low temperature (292–296K for the TAMU data and 303–305 K for the GT data) and present an internally consistent picture of the effect of both temperature and pressure on flame speed at stoichiometric conditions. The small discrepancy between measurements at low temperatures is indicative of the sensitivity of flame speed to reactant temperature.

The model agrees well with experimental values, reproducing the effect of increasing methane concentration, increasing temperature and increasing pressure. The simulations are extended across the full range of values, from pure methane to pure ethane or propane. The variation in flame speed is seen to be nonlinear with fuel-composition. Small amounts of higher hydrocarbon fuels to methane increase the flame speed more than would be expected based on a simple linear superposition of the pure fuel flame speeds. This general behavior is consistent with previous studies of hydrocarbon fuel blends [55].

Further analysis on the effect of blending ratio was performed in the form of a modeling sensitivity analysis. The results are shown in Figure 13, which depicts the ten most sensitive reactions for a variety of different fuel mixtures from pure methane, to 60% methane 40% ethane, 60% methane 40% propane and finally to pure ethane and pure propane. The analysis centered on the effect of each reaction on the calculated mass flow rate, and was performed at a stoichiometry of 1.0, T<sub>u</sub> = 298K and P<sub>i</sub> = 5.0 atm. In all cases the O<sub>2</sub>/He ratio was maintained at 1:6.

The dominant feature of Figure 13 is the importance of the reaction  $H+O_2 \rightleftharpoons O+OH$ , across all the examined fuel blends. This feature is to be expected as this reaction is the most

important chain branching process in high temperature combustion kinetics. This reaction shows the highest sensitivity for the pure methane case, and decreases with increasing ethane concentration. This feature is also present when moving from pure methane to pure propane.

The primary reaction responsible for the conversion of carbon monoxide to carbon dioxide at high temperatures,  $\text{CO} + \text{OH} \rightleftharpoons \text{CO}_2 + \text{H}$ , is the next most important reaction. The promoting effect of this reaction is effectively constant over all conditions of this analysis, and would perhaps vary more with stoichiometry than with blending fractions.

The final feature of this analysis to highlight is the sparsity of reactions involving the parent fuel molecules. No reactions involving ethane or propane are found in the ten most sensitive reactions at this condition, with only one abstraction reaction from methane showing sufficient sensitivity. However the recombination reaction between methyl radical and hydrogen atom to form methane is important under all 5 blending regimes. These points highlight the importance of small species chemistry to the high temperature combustion of larger hydrocarbon fuels, with accurate descriptions of the chemistry of methyl, hydroxyl and formyl radicals, together with atomic species, hydrogen and oxygen, extremely pertinent.

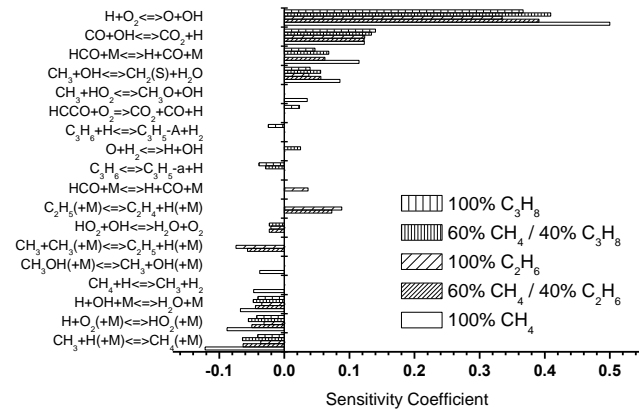


**Figure 13: A flow rate sensitivity plot comparing different blends of  $\text{CH}_4$ ,  $\text{C}_2\text{H}_6$  and  $\text{C}_3\text{H}_8$  with  $\text{O}_2 / \text{He}$  (1:6) diluent. Analysis performed at  $\phi = 1.0$ ,  $T_u = 298\text{K}$ , and  $P_i = 5.0 \text{ atm}$ .**

### SUMMARY

Two flame speed measurement facilities at TAMU and GT have been used to record flame speeds at unburned gas temperatures of  $\sim 300 \text{ K}$  and  $600\text{--}650 \text{ K}$  and at pressures of 1-, 5- and 10-atm. Agreement between the experimental data and results from previous work is quite good for the cases where overlapping data are available. The results show a strong sensitivity to reactant temperature. Even small increases in initial temperature (e.g., from  $295\text{K}$  to  $305\text{K}$ ) produce measurably higher flame speeds.

In addition, an improved C4 chemical kinetics model was presented, with comparisons between the model and the experimental data. Generally, good agreement is seen between the model and the experimental results. Systematic discrepancies were found between the modeling and jet flame data in cases of He diluted oxidizers. The experimental data produce peak laminar flame speeds at leaner mixtures than predicted by the model. Still, the model results are able to capture the temperature and pressure dependence of the laminar flame speed across the full range of pressures and temperatures examined here. In addition, it provides accurate predictions of flame speed for both pure fuels and for the binary mixtures of methane-ethane and methane-propane tested.

### ACKNOWLEDGMENTS

This work was supported primarily by Rolls-Royce Canada.

### REFERENCES

- [1] Lowry, W., de Vries, J., Krejci, M., Petersen, E., Serinyel, Z., Metcalfe, W., Curran, H., and Bourque, G., 2011 "Laminar Flame Speed Measurements and Modeling of Pure Alkanes and Alkane Blends at Elevated Pressures," *Journal of Engineering for Gas Turbines and Power*, in press.
- [2] Lieuwen T C, Yang V. Combustion instabilities in gas turbine engines: Operational experience, fundamental mechanisms, and modeling; 2005. (Danvers, MA: AIAA)
- [3] Bradley D., Hicks R. A., Lawes M., Sheppard C. G. W., Woolley R., 1998, "The Measurement of Laminar Burning Velocities and Markstein Numbers for Iso-octane-Air and Iso-octane-n-Heptane-Air Mixtures at Elevated Temperatures and Pressures in an Explosion Bomb," *Combustion and Flame* 115 pp. 126–144.
- [4] Bourque G., Healy D., Curran H., Zinner C., Kalitan D., de Vries J., Aul C., and Petersen E., 2008 "Ignition and Flame Speed Kinetics of Two Natural Gas Blends with Higher Levels of Heavier Hydrocarbons," ASME Turbo Expo (2008) Paper nr. GT2008-51344.
- [5] Rozenchan G., Zhu D. L., Law C. K., and Tse S. D., 2002 "Outward Propagation, Burning Velocities, and Chemical Effects of Methane Flames up to 60 atm," *Proceedings of the Combustion Institute* 29, pp. 1461–1469.
- [6] Natarajan, J., Kochar, Y., Lieuwen, T., and Seitzman, J., 2009 "Pressure and Preheat Dependence of

Laminar Flame Speeds of H<sub>2</sub>/CO/CO<sub>2</sub>/O<sub>2</sub>/He Mixtures,” Proceedings of the Combustion Institute 32, pp. 1261-1268.

- [7] Vu. T. M., Park, J., Kwon, O. B., Bae, D. S., Yun, J. H., and Keel, S. I., 2010 “Effects of Diluents on Cellular Instabilities in Outwardly Propagating Spherical Syngas-Air Premixed Flames,” International Journal of Hydrogen Energy 35, pp. 3868-3880.
- [8] Ó Conaire M., Curran H.J., Simmie J.M, Pitz W.J., and Westbrook C.K., 2004, “A Comprehensive Modeling Study of Hydrogen Oxidation,” International Journal of Chemical Kinetics 36 pp. 603–622.
- [9] Petersen E.L., Kalitan D.M., Simmons S., Bourque G., Curran H.J., and Simmie J.M., 2007, “Methane/Propane Oxidation at High Pressures: Experimental and Detailed Chemical Kinetic Modeling,” Proceedings of the Combustion Institute 31, pp. 447–454.
- [10] Healy D., Curran H.J., Dooley S., Simmie J.M., Kalitan D.M., Petersen E.L., and Bourque G., 2008, “Methane/Propane Mixture Oxidation at High Pressures and at High, Intermediate and Low Temperatures,” Combustion and Flame 155 pp. 451–461.
- [11] Healy D., Curran H.J., Simmie J.M., Kalitan D.M., Zinner C.M., Barrett A.B., Petersen E.L., and Bourque G., “Methane/Ethane/Propane Mixture Oxidation at High Pressures and at High, Intermediate and Low Temperatures,” 2008, Combustion and Flame, 155 pp. 441–448.
- [12] Natarajan, J., Lieuwen, T., and Seitzman, J., 2007 “Laminar Flame Speeds of H<sub>2</sub>/CO Mixtures: Effect of CO<sub>2</sub> Dilution, Preheat Temperature, and Pressure,” Combustion and Flame 151 pp. 104–119.
- [13] de Vries J., “A study on spherical expanding flame speeds of methane, ethane, and methane/ethane mixtures at elevated pressures,” PhD Dissertation, Texas A&M University, 2009
- [14] Settles G. S., 2006 Schlieren and Shadowgraph Techniques, Springer, Heidelberg, Germany
- [15] CHEMKIN-PRO, Reaction Design, San Diego, 2008.
- [16] Healy D., Curran H.J., Petersen E.L., Aul C., Donato N., Zinner C., and Bourque G., 2009, “n-Butane: Ignition Delay Measurements at High Pressure and Detailed Chemical Kinetic Simulations,” Combustion and Flame, 157 pp. 1526–1539.
- [17] Healy D., Curran H.J., Petersen E.L., Aul C., Donato N., Zinner C., and Bourque G., 2009, “Isobutane: Ignition Delay Time Measurements at High Pressure and Detailed Chemical Kinetic Simulations,” Combustion and Flame, 157 pp. 1540–1551.
- [18] Hong Z., Davidson D.F., Hanson R.K., “An Improved H<sub>2</sub>/O<sub>2</sub> mechanism based on recent shock tube/laser absorption measurements”, Combustion and Flame, in press.
- [19] You X., Wang H., Goos, E., Sung, C-H., Klippenstein, S.J., 2007, “Reaction Kinetics of CO+HO<sub>2</sub>→Products: Ab Initio Transition State Theory Study with Master Equation Modeling”, Journal of Physical Chemistry A, 111, pp. 4031–4042.
- [20] [http://www.me.berkeley.edu/gri\\_mech/](http://www.me.berkeley.edu/gri_mech/)
- [21] Baulch D.L., Cobos C.J., Cox R.A., Esser C., Frank P., Just Th., Kerr J.A., Pilling M.J., Troe J., Walker R. W., Warnatz J., 1992, “Evaluated Kinetic Data for Combustion Modelling”, J. Phys. Chem. Ref. Data 21, pp. 411–429.
- [22] Klippenstein S.J., Miller J.A. and Harding L.B., “Resolving the Mystery of Prompt CO<sub>2</sub>: The HCCO+O<sub>2</sub> Reaction”, 2002, Proceedings of the Combustion Institute, Volume 29, pp. 1209–1217.
- [23] Aguilera-Iparraguirre J., Curran H.J., Klopper W., Simmie J.M., “Accurate Benchmark Calculation of the Reaction Barrier Height for Hydrogen Abstraction by the Hydroperoxyl Radical from Methane. Implications for C<sub>n</sub>H<sub>2n+2</sub> where n = 2–4”, 2008, Journal of Physical Chemistry A 112(30) pp. 7047–7054.
- [24] (a) Feng, Y., Niiranen J.T., Bencsura A., Knyazev V.D., Gutman D., “Weak collision effects in the reaction C<sub>2</sub>H<sub>5</sub> = C<sub>2</sub>H<sub>4</sub> + H”, Journal of Physical Chemistry, 97(4):871–880, 1993. (b) Saxena P. and Williams. F.A., “Work in Progress Communication”, Center for Energy Research, 2005.
- [25] Stewart, P.H., Larson C.W., and Golden D. M., 1989, “Pressure and Temperature Dependence of Reactions Proceeding via a Bound Complex. 2. Application to 2CH<sub>3</sub> → C<sub>2</sub>H<sub>5</sub> + H”, Combustion and Flame 75 pp. 25–31.

- [26] DeSain J.D., Klippenstein S.J., Miller J. A., Taatjes C.A., 2003, "Measurements, Theory, and Modeling of OH Formation in Ethyl + O<sub>2</sub> and Propyl + O<sub>2</sub> Reactions", *Journal of Physical Chemistry A*, 107 pp. 4415–4427.
- [27] Senosiain J.P., Klippenstein S.J., Miller J.A., 2006, "Pathways and Rate Coefficients for the Decomposition of Vinyloxy and Acetyl Radicals", *Journal of Physical Chemistry A*, 110 pp. 5772–5781.
- [28] Baulch D. L., Bowman C. T., Cobos C. J., Cox R. A., Just Th., Kerr J. A., Pilling M. J., Stocker D., Troe J., Tsang W., Walker R. W., Warnatz J., 2005, *J. Phys. Chem. Ref. Data* 34 pp. 757.
- [29] Marinov N.M., and Malte P.C., 1995, "Ethylene oxidation in a well-stirred reactor.", *International Journal of Chemical Kinetics*, 27(10) pp.957–986.
- [30] Pitz, W.J., Personal Communication.
- [31] Marinov N. M., Pitz W.J., Westbrook C.K., Vincitore A.M., Castaldi M.J., Senkan S.M., 1998, *Combustion and Flame* 114 pp. 192–213.
- [32] Miller J.A., Klippenstein S.J., 2004, "The H+C<sub>2</sub>H<sub>2</sub> (+M)↔C<sub>2</sub>H<sub>3</sub> (+M) and H+C<sub>2</sub>H<sub>2</sub> (+M)↔C<sub>2</sub>H<sub>5</sub> (+M) reactions: Electronic structure, variational transition state theory, and solutions to a two-dimensional master equation", *Phys. Chem. Chem. Phys.*, 6 pp. 1192–1202. Marinov N. M., Pitz W.J., Westbrook C.K., Vincitore A.M., Castaldi M.J., Senkan S.M., 1998, *Combustion and Flame* 114 pp. 192–213.
- [33] Kochar Y., Vaden S., Lieuwen T., Seitzman J., "Laminar Flame Speed of Hydrocarbon Fuels with Preheat and Low Oxygen Content", AIAA-2010-778.
- [34] Aung K. T., Tseng L. K., Ismail M. A., and Faeth G. M., 1995 "Response to Comment by S. C. Taylor and D. B. Smith on "Laminar Burning Velocities and Markstein Numbers of Hydrocarbon/Air Flames," *Combustion and Flame* 102 pp. 526–530.
- [35] Hassan M. I., Aung K. T., and Faeth G. M., 1998 "Measured and Predicted Properties of Laminar Premixed Methane/Air Flames at Various Pressures," *Combustion and Flame* 115 pp. 539–550.
- [36] Vagelopoulos C. M. and Egolfopoulos F. N., 1998 "Direct Experimental Determination of Laminar Flame Speeds," *Proceedings of the Combustion Institute* 27, pp. 513–519.
- [37] Gu X. J., Haq M. Z., Lawes M., and Woolley R., 2000 "Laminar Burning Velocity and Markstein Lengths of Methane-Air Mixtures," *Combustion and Flame* 121 pp. 41–58.
- [38] Rozenchan G., Zhu D. L., Law C. K., and Tse S. D., 2002 "Outward Propagation, Burning Velocities, and Chemical Effects of Methane Flames up to 60 atm," *Proceedings of the Combustion Institute* 29, pp. 1461–1469.
- [39] Bosschaart K. J., de Goey L. P. H., and Burgers J. M., 2004 "The Laminar Burning Velocity of Flames Propagating in Mixtures of Hydrocarbons and Air Measured with the Heat Flux Method," *Combustion and Flame* 136 pp. 261–269.
- [40] Tahtouh T., Halter F., and Mounaim-Rousselle C., 2009 "Measurement of Laminar Burning Speeds and Markstein Lengths Using a Novel Methodology," *Combustion and Flame* 156 pp. 1735–1743.
- [41] Konnov A. A., Dyakov I. V., and De Ruyck J., 2003 "Measurement of Adiabatic Burning Velocity in Ethane-Oxygen-Nitrogen and in Ethane-Oxygen-Argon Mixtures," *Experimental Thermal and Fluid Science* 27 pp. 379–384.
- [42] Jomaas G., Zheng X. L., Zhu D. L., and Law C. K., 2005 "Experimental Determination of Counterflow Ignition Temperatures and Laminar Flame Speeds of C<sub>2</sub>-C<sub>3</sub> Hydrocarbons at Atmospheric and Elevated Pressures," *Proceedings of the Combustion Institute* 30, pp. 193–200.
- [43] Dyakov I. V., De Ruyck J., Konnov A. A., 2007, "Probe Sampling Measurements and Modeling of Nitric Oxide Formation in Ethane + Air Flames," *Fuel* 86 pp. 98–105.
- [44] Zhao Z., Kazakov A., Li J., and Dryer F. L., 2004 "The Initial Temperature and N<sub>2</sub> Dilution Effect on the Laminar Flame Speed of Propane/Air," *Combustion Science and Technology* 176 pp. 1705–1723.
- [45] Gibbs G. J. and Calcote H.F., 1959, "Effect of Molecular Structure on Burning Velocity," *Journal of Chemical and Engineering Data*, 4, No. 3 pp. 226–237.
- [46] Dugger, G.L. "Effect of initial mixture temperature on flame speed of methane-air, propane-air, and ethylene-air mixtures", NACA-Report-1061, 1952.

- [47] van Maaren A. and de Goey L. P. H., 1994, "Stretch and the Adiabatic Burning Velocity of Methane-and Propane-Air Flames," *Combust. Sci. Technol.* 102 309–314.
- [48] Hassan M. I., Aung K. T., Kwon O. C., and Faeth G. M., 1998 "Properties of Laminar Premixed Hydrocarbon/Air Flames at Various Pressures," *Journal of Propulsion and Power* 14 pp. 479–488.
- [49] Metghalchi M. and Keck J. C., 1980, "Laminar Burning Velocity of Propane-Air Mixtures at High Temperature and Pressure," *Combustion and Flame* 38 pp. 143–154.
- [50] Zhou M. and Garner C.P., 1996, "Direct Measurements of Burning Velocity of Propane-Air Using Particle Image Velocimetry," *Combustion and Flame* 106 pp. 363–367.
- [51] Law C. K. and Kwon O. C., 2004 "Effects of Hydrocarbon Substitution on Atmospheric Hydrogen-Air Flame Propagation," *International Journal of Hydrogen Energy* 29 pp. 867–879.
- [52] Tang C., Zheng, J., Huang, Z., Wang, J., 2010, "Study on nitrogen diluted propane-air premixed flames at elevated pressures and temperatures", *Energy Conversion and Management* 51 pp. 288–295.
- [53] Tseng L.K., Ismail, M.A., Faeth, G.M. 1993, "Laminar burning velocities and Markstein numbers of hydrocarbon/air flames", *Combustion and Flame* 95(4) pp. 410–426.
- [54] Razus, D., Oancea, D., Brinzea, V., Mitu, M., Movileanu, C., 2010, "Experimental and computed burning velocities of propane-air mixtures", *Energy Conversion and Management* 51 pp. 2979–2984.
- [55] Hirawawa, T., Sung, C. J., Joshi, A., Yang, Z., Wang, H., Law C. K., 2002, "Determination of Laminar Flame Speeds Using Digital Particle Image Velocimetry: Binary Fuel Blends of Ethylene, n-Butane, and Toluene", *Proceedings of the Combustion Institute* 29 pp. 1427–1434.